An Efficient and Accurate Approximation to the Balance Wind with Application to Non-Elliptic Data

JAN PAEGLE AND JULIA N. PAEGLE

Department of Meteorology, University of Utah, Salt Lake City, Utah 84112

(Manuscript received 2 August 1974, in revised form 19 September 1974)

ABSTRACT

An efficient alternative to the customary balance equation solution procedures is described which gives very similar solutions for those cases when the balance equation is elliptic. This alternative invokes some assumptions that are not usually applied to the nonlinear balance equation, but which are justified by comparisons with the standard solutions to the balance equation in both rectangular and spherical geometries. The solution tends toward a flow with zero absolute vorticity as the pressure field tends toward configurations for which the balance equation is non-elliptic. Such non-elliptic pressure fields correspond to force fields with sufficient positive divergence with respect to space to generate flow divergence. In this case a non-divergent balanced solution may not exist, and is physically meaningless if it does exist, but a reasonable divergent balanced solution can be obtained by the proposed technique.

1. Introduction

Miyakoda (1956) and Shuman (1957) have presented methods for the solution of the complete nonlinear balance equation. The nonlinearity of the equation complicates the solution procedures, and sometimes the balance equation is linearized by approximating the entire nonlinear term by its geostrophic value (Krishnamurti, 1968). This produces considerable simplification in the computations, but the results represent poor approximations to gradient solutions in strongly rotating circular flows. The approach we suggest is to apply this type of linearization only to the deformation components of the nonlinear terms. The solutions of the resulting equations can be obtained quite efficiently, and they are good approximations to the fully nonlinear balance equation solution.

This method gives a solution that corresponds to an early approximation of the solutions proposed by Shuman (1957) and Miyakoda (1956) but which has the following advantages:

i) The kinematic properties of the flow, such as divergence, vorticity, and deformation, are independent of flow boundary conditions. This is of importance in small-domain localized diagnostic studies for which boundary conditions are not known.

ii) The ellipticity condition of the governing equations corresponds exactly to the condition of non-negative absolute vorticity. This condition is easy to motivate, unlike the ellipticity condition of the customary balance equation, which has no clear cut physical interpretation.

iii) The balanced steady-state *divergent* flow suggested by this approach is a realizable steady-state limit to the time dependent equations. The customary balance equation may also be forced to be elliptic by introducing the appropriate divergence. This fact seems not to have been previously used. However, the resulting divergent flow field has no apparent general physical interpretation, other than a solvability requirement which doesn't involve a modification of the pressure data.

iv) This scheme is significantly more economical than the solution of the customary balance equation, but shows remarkable resemblance to the solution of the latter. Stronger linearizations, such as those described by Krishnamurti (1968), or contained in the steady-state subset of Fjørtoft's (1962) equations also result in economical algorithms. In the particular case of gradient flow, these linearizations approximate the centripetal term with a geostrophic value, and this results in substantial vorticity errors in strongly rotating systems. On the other hand, the proposed solution reproduces gradient flow exactly.

The suggested approach may be of use in other applications in which the balance equation is commonly used. In particular, this method might prove a useful diagnostic tool for certain anomalous divergent wind patterns like those reported by Krishnamurti (1971) and Syōno (1948).

The partial linearization mentioned above and the assumption that the motion is steady leads to a solution

procedure whereby the flow can be obtained algebraically (Section 2). The correspondence of boundary value differential equation solutions to algebraic solutions is discussed in Section 3.

Section 4 discusses a physically plausible divergent solution obtained from this method. In Section 5, solutions by the proposed algorithm are compared with those obtained from the customary nonlinear balance equation for both rectangular and spherical geometries.

2. Algebraic solution

In spherical coordinates the divergence equation may be written as

$$\frac{dD}{dt}+\frac{1}{2}(A^2+B^2+D^2-\xi^2)-f\xi+\nabla^2\Phi=-\beta u-\frac{v^2+u^2}{a^2}-\frac{2\tan\phi}{a^2}\left[uu_\phi+vv_\phi+\frac{1}{\cos\phi}(uv_\lambda-vu_\lambda)\right], \quad (1)$$

where

$$D=\frac{1}{a\cos\phi}\left[\frac{\partial}{\partial\phi}(v\cos\phi)+\frac{\partial u}{\partial\lambda}\right]$$

$$A=\frac{1}{a\cos\phi}\left[\frac{\partial v}{\partial\lambda}+\frac{\partial}{\partial\phi}(u\cos\phi)\right]$$

$$B=\frac{1}{a\cos\phi}\left[\frac{\partial}{\partial\phi}(v\cos\phi)-\frac{\partial u}{\partial\lambda}\right]$$

$$\xi=\frac{1}{a\cos\phi}\left[\frac{\partial v}{\partial\lambda}-\frac{\partial}{\partial\phi}(u\cos\phi)\right]$$

$$u=a\cos\phi\frac{d\lambda}{dt}$$

$$v=a\frac{d\phi}{dt}$$

a = earth radius

ϕ = latitude

λ = longitude

Φ = geopotential

$$\nabla^2\Phi=\frac{1}{a^2}\left[\frac{1}{\cos^2\phi}\frac{\partial^2\Phi}{\partial\lambda^2}+\frac{\partial^2\Phi}{\partial\phi^2}\right]-\frac{\tan\phi}{a^2}\frac{\partial\Phi}{\partial\phi}.$$

Eq. (1) leads to the balance equation when dD/dt is neglected. This is customarily done to filter out gravitational waves (Thompson, 1956).

Eq. (1) can be rewritten as

$$\xi^2+2f\xi-(A^2+B^2+D^2+2\nabla^2\Phi-2G)=0, \quad (2)$$

where

$$G=-\beta u-\frac{v^2+u^2}{a^2}-\frac{2\tan\phi}{a^2}\left[uu_\phi+vv_\phi+\frac{1}{\cos\phi}(uv_\lambda-vu_\lambda)\right].$$

Eq. (2) can now be solved for ξ, similarly to the approach of Miyakoda (1956) and Shuman (1957),

$$\xi=-f\pm(f^2+A^2+B^2+D^2+2\nabla^2\Phi-2G)^{\frac{1}{2}}. \quad (3)$$

From the definitions above it can be easily seen that

$$\begin{aligned}\frac{\partial v}{\partial\phi}&=\frac{a}{2}(D+B)+v\tan\phi\\ \frac{\partial u}{\partial\phi}&=\frac{a}{2}(A-\xi)+u\tan\phi\\ \frac{\partial u}{\partial\lambda}&=\frac{a\cos\phi}{2}(D-B)\\ \frac{\partial v}{\partial\lambda}&=\frac{a\cos\phi}{2}(A+\xi).\end{aligned} \quad (4)$$

For the case of non-divergence, $D=0$ and the wind is given by $\mathbf{V}=\mathbf{k}\times\nabla\psi$. Miyakoda and Shuman (loc. cit.) have solved (3) for Cartesian coordinates by iterating in the streamfunction.

We will show later that replacing the deformation components A and B, as well as the metric and beta terms by their geostrophic values, gives a close approximation to the solution of (3). This corresponds to an early approximation in Miyakoda's and Shuman's iterative methods, but it has several advantages which will be discussed in later sections.

The u and v components may be obtained from the steady state equations of motion. The impact of this simplification is further discussed in Section 5. The equations

$$\frac{uu_\lambda}{a\cos\phi}+\frac{v u_\phi}{a}-fv=-\frac{\Phi_\lambda}{a\cos\phi}+uv\frac{\tan\phi}{a}\equiv E1 \quad (5)$$

$$\frac{uv_\lambda}{a\cos\phi}+\frac{v v_\phi}{a}+fu=-\frac{\Phi_\phi}{a}-u^2\frac{\tan\phi}{a}\equiv E2 \quad (6)$$

can be solved for u and v in terms of the first flow derivatives as follows:

$$u=\{E2(f-u_\phi/a)a\cos\phi+E1v_\phi\cos\phi\}/W \quad (7)$$

$$v=\{-E1(v_\lambda+fa\cos\phi)+E2u_\lambda\}/W, \quad (8)$$

where

$$W=\{-(u_\phi/a-f)[v_\lambda/(a\cos\phi)+f]a\cos\phi\}+u_\lambda v_\phi/a.$$

Thus, by approximating the quantity under the radical and metrical terms by their geostrophic values,

the vorticity and flow derivatives can be obtained from (3) and (4) for a given pressure field. The wind components can then be obtained directly from (7) and (8). This method does not involve the solution of any differential equation and, therefore, is not directly dependent on boundary specifications. This advantage can also be retained by leaving all metric terms appearing in all the components of (3) and (4), as well as the beta term in their nongeostrophic form. Using the values of u and v given by (7) and (8), the metrical terms needed in (3), (4) and in the E1 and E2 terms of (7) and (8) can be updated for new solution values. Iterating this procedure leads to a rapidly converging sequence of solutions for u, v, $\partial u/\partial\phi$, $\partial v/\partial\phi$, $\partial u/\partial\lambda$, $\partial v/\partial\lambda$ away from the poles. The results obtained from this method are practically the same as those obtained by approximating the metrical terms by their geostrophic values.

3. Algebraic solutions and differential equation solutions

The algebraic procedure described in the previous section can be used to obtain the kinematics of the flow field for a given geopotential field *independently* of boundary conditions on the flow. The important consequences of this fact, as well as its origin, are more clearly apparent if we consider a rectangular geometry, and ignore all terms of the equation arising from the earth's sphericity. This simplification modifies the quantitative results somewhat, but not the substance of the following arguments.

In a rectangular geometry, with coordinates x and y, the fully nonlinear balance equation is

$$-2[-\psi_{xx}\psi_{yy}+(\psi_{xy})^2]+f\nabla^2\psi=\nabla^2\Phi, \tag{9}$$

while the version corresponding to (2) is

$$\xi^2+2f\xi-(A^2+B^2+D^2)=2\nabla^2\Phi, \tag{10}$$

where now

$$\begin{aligned}\xi&=v_x-u_y\\ D&=v_y+u_x\\ A&=v_x+u_y\\ B&=v_y-u_x.\end{aligned} \tag{11}$$

For the case of no divergence ($D=0$) the deformation terms in (11) are approximated by their geostrophic values, that is,

$$A=A_g=(\Phi_{xx}-\Phi_{yy})/f \quad \text{and} \quad B=B_g=2\Phi_{xy}/f, \tag{12}$$

to obtain an algebraic solution for u, v, and their derivatives, as in the last section.

As discussed then, the flow derivatives can be explicitly obtained from (11) after solving (10) for ξ, using these deformation values and the non-divergent condition, $D=0$.

It is apparent that the vorticity and rate of deformation are independent of the boundary conditions on ψ, even if (10) is solved for ξ and if ψ is subsequently obtained from (17) below. Thus, the independence of these kinematic properties from flow boundary conditions arises as a consequence of the linearization of the deformation terms in the balance equation.

Invoking the steady state assumption for the component equations of motion, as in the last section, we obtain for rectangular coordinates

$$u=[-\Phi_y(u_y-f)+\Phi_x v_y]/\{(v_x+f)(u_y-f)-u_x v_y\} \tag{13}$$

$$v=\{\Phi_y u_x-\Phi_x(v_x+f)\}/\{(u_y-f)(v_x+f)-u_x v_y\}. \tag{14}$$

There is no guarantee that the vorticity obtained from (13) and (14) matches that given by ξ. ξ is obtained under the condition of $dD/dt=0$ while u and v in (13) and (14) are obtained under the stronger condition of steady flow. We note here that this inconsistency can be avoided by solving for u and v, as follows:

$$u=-\frac{\partial\psi}{\partial y} \tag{15}$$

$$v=\frac{\partial\psi}{\partial x}, \tag{16}$$

where ψ is obtained from the solution of

$$\nabla^2\psi=\xi \tag{17}$$

and where ξ is obtained from the solution of (10).

In this case boundary values on ψ are required, and u and v become dependent on these boundary conditions, even though the vorticity is not. The boundary conditions would be given by

$$\frac{\partial\psi}{\partial s}=v_n, \tag{18}$$

where s is the distance around the boundary curve and v_n is the appropriate velocity component normal to the boundary curve. Integrating this around the boundary would give the boundary condition on ψ, if v_n is known. Since the object of solution is the velocity field, v_n is not usually known and specification of boundary conditions introduces some indeterminacy into the result.

The degree of such indeterminacy is smaller for (10) than it is for (9). Only the u and v fields are indeterminate for the latter, while these, as well as the vorticity, are determined by the (usually) unknown boundary conditions needed for (9). As two extreme examples of the dependence of the solution of (9) on boundary values, we consider a rectangular boundary and a circular boundary with the flow driven by the same pressure field in both cases.

The boundary conditions of the first example are diagrammed in Fig. 1a. For a geopotential field,

$$\Phi=-2B^2(x^2+y^2), \quad B \text{ real}, \tag{19}$$

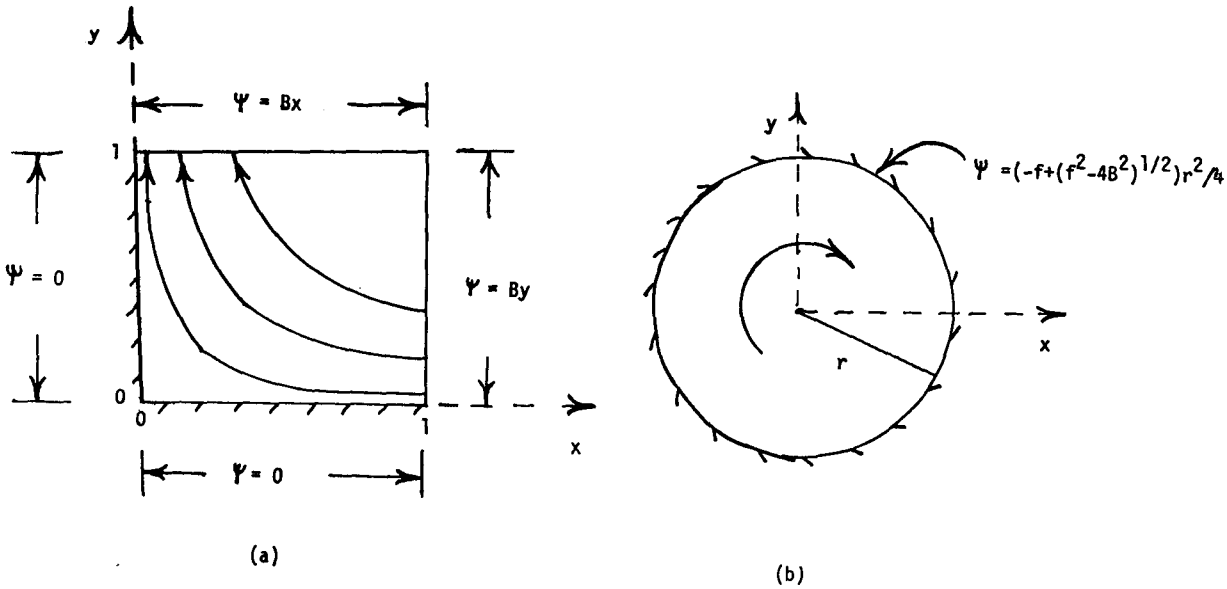

FIG. 1. (a) Square domain within which the balance equation is solved as discussed in the text. The imposed boundary conditions are indicated on the sides of the square which has corners at (0, 0), (0, 1), (1, 1) and (1, 0). Curved arrows denote sample streamlines of the balanced flow. (b) Circular domain within which the balance equation is solved as discussed in the text. The imposed boundary condition of no flow through the circle at radius r is indicated. The curved arrow represents a sample streamline of the balanced flow.

the solution of (9) satisfying the boundary conditions of Fig. 1a is

$$\psi = 2Bxy. \tag{20}$$

For this case,

$$\psi_{xx} = \psi_{yy} = 0, \quad \psi_{xy} \neq 0. \tag{21}$$

While (20) represents a solution to (9), it has the peculiar characteristic that the resulting flow is independent of the rotation of the system.

The boundary conditions of the second example are diagrammed in Fig. 1b and the solution for the same geopotential field (19) is

$$\psi = [f + (f^2 - 16B^2)^{\frac{1}{2}}](x^2 + y^2)/4. \tag{22}$$

In this case,

$$\psi_{xx} = \psi_{yy} \neq 0, \quad \psi_{xy} = 0. \tag{23}$$

The first example has deformation but no rotation, while the second has rotation but no deformation, even though it is driven by the same pressure field. Clearly the position and the nature of the boundary conditions have great impact on the type of balanced flow. Of equal importance is the fact that even for a fixed type of boundary condition, variation of the boundary location produces flow variations which are not negligible. In real 500-mb data experimentation we have found that the balanced winds can vary by 2–3 m/s in response to changes of the position of boundary points at which the geostrophic streamfunction is imposed. In some cases this variation is on about the same order as the difference of the balance solution from the geostrophic solution.

The main point of this discussion relates to circumstances when the region of interest is a localized domain. Then the solution of the balance equation requires artificial inflow-outflow boundary conditions, and these (unknown) conditions to a large extent determine the interior flow. It is then convenient to have a method for obtaining the flow which does not require guesswork concerning flow boundary conditions. In this sense the proposed method might be more suitable than the standard method for local diagnostic studies.

4. The ellipticity condition and divergent balanced flows

In the algebraic solution for ξ, the radical of (3) must be real in order that a meaningful solution exists. Considering a similar constraint in the rectangular geometry used in the last section (Miyakoda, 1956) leads to the following alternatives:

1) The pressure field should be such as to keep the radical real. This is equivalent to an ellipticity condition on the pressure data.
2) Some divergence must exist so that the radical remains real.

The first alternative restricts the nature of the pressure field while the second demands that the condition of non-divergent flow be relaxed, and leaves open the question of how the divergent flow component can be obtained. In this section we will first substantiate the above statements in rectangular geometry, and second, indicate how the second alternative can be incorporated,

The condition of real radical reduces to

$$f^2+(B^2+A^2+D^2)+2\nabla^2\Phi\geq 0. \tag{24}$$

It is easy to show that (24) is also the ellipticity condition for (10) by applying A'rnason's (1958) analyses to (10). If the deformation components A and B are not linearized, the ellipticity condition is:

$$f^2+D^2+2\nabla^2\Phi>0,$$

as shown by Miyakoda (1956). Thus, for the algebraic method, the domain where the balance equation is elliptic coincides exactly with the domain where the algebraic solution for ξ can exist.

When the force field has sufficient divergence to render the balance equation non-elliptic and (24) is not satisfied, the data field must be modified, or some divergence must be permitted. The former alternative has always been chosen in the past, on the basis that the data modifications are within the errors of observations, but there may be situations when the latter alternative would be more correct. The difficulty is that a more complete divergence equation than that represented by the balance equation is required, if divergent solutions are allowed.

Therefore, we consider, for the purpose of interpretation, the complete divergence, vorticity, and deformation equations in Cartesian coordinates, neglecting all terms arising from the earth's sphericity. Although these simplifications affect the quantitative results over a large region (somewhat) they are good approximations for a localized domain. The resulting equations are

$$\frac{dD}{dt}=\frac{1}{2}(\xi+f)^2-\frac{f^2}{2}-\frac{1}{2}(A^2+B^2+D^2)-\nabla^2\Phi \tag{25}$$

$$\frac{dB}{dt}=-DB-f(A-A_g) \tag{26}$$

$$\frac{dA}{dt}=-DA+f(B-B_g) \tag{27}$$

$$\frac{d\xi}{dt}=-(\xi+f)D, \tag{28}$$

where $A=v_x+u_y$, $B=v_y-u_x$, $A_g=(1/f)[\Phi_{xx}-\Phi_{yy}]$, $B_g=(2/f)\Phi_{xy}$.

With force fields such that $\nabla^2\Phi<-f^2/2$ and this, as well as B_g and A_g, constant in space, the time dependent solution will be characterized by D, A, B, and ξ constant throughout the field. Such an assumption is already implicit in the algebraic solution for the non-divergent case, which also satisfies (25)–(27) only with neglect of advective affects. While this seems a rather strong constraint, the solutions obtained from actual data appear to justify it.

Using this assumption, the total time derivatives can be replaced by local time derivatives. Then it is possible to verify that a steady state results such that

$$\xi=-f \tag{29}$$

$$A^2+B^2=(A_g^2+B_g^2)/(1+D^2/f^2) \tag{30}$$

$$D^2=-\{f^2+2\nabla^2\Phi+(A_g^2+B_g^2)/(1+D^2/f^2)\}, \tag{31}$$

or

$$D^2=-(f^2+\nabla^2\Phi)\pm f\left[\left(\frac{\nabla^2\Phi}{f}\right)^2-(A_g^2+B_g^2)\right]^{\frac{1}{2}}. \tag{32}$$

Thus, for all cases for which $D^2\ll f^2$,

$$D\doteq\{-(f^2+2\nabla^2\Phi+A_g^2+B_g^2)\}^{\frac{1}{2}} \tag{33}$$

For large D it is more appropriate to use (32) to obtain D.

It is noteworthy that (32) or (33) are the same conditions which render

i) Eq. (10) elliptic when A^2+B^2 is given by (30)
ii) ξ real when (10) is solved algebraically for ξ for any pressure field.

These conclusions can be extended to spherical coordinates with the incorporation of geostrophic values for the metrical terms. Thus, this method allows one to compute the divergence field that ensues from divergent force fields associated with non-elliptic data. It should be noted that the vorticity and, therefore, the rotational components of the wind will be the same whether the equation is made elliptic by introducing divergence or modifying Φ. Further discussion of situations for which these results may be of particular applicability and benefit is deferred to the next section.

5. Numerical experiments

Three types of experiments were conducted. The first is for a rectangular geometry in a situation with exact solutions for the fully nonlinear balance equation (9) in the elliptic case. The second experiment is for a similar case with a pressure field which is locally non-elliptic. The third experiment applies to the spherical case and mid-winter data on a grid which covers most of the Northern Hemisphere.

a. Rectangular coordinates, elliptic data

Exact solutions are available in the rectangular geometry and this fact minimizes the effects of truncation error in comparison of results. It is a straightforward matter to verify that, for a pressure field given by,

$$\Phi=-\frac{\bar{V}^2}{4}\{[1-2\cos^2(ky)]+[1-2\cos^2(kx)]\}$$

$$+\frac{\beta\bar{V}}{2k^2}\sin(kx)\cos(ky)-\frac{f\bar{V}}{k}\sin(kx)\sin(ky), \quad (34)$$

and boundary conditions specifying

$$\psi=0 \quad \text{on} \quad kx=0,\ 2\pi,\ ky=0,\ 2\pi, \quad (35)$$

the solution of the balance equation (9) is

$$\psi=-(\bar{V}/k)\sin(kx)\sin(ky). \quad (36)$$

Figure 2 displays analyses of isolines of Φ and ψ for various values of $\bar{V}$ and fixed f and k. As the parameter $\bar{V}$ increases, the nonlinearity of the balance equation becomes increasingly important, and for a wavelength of 6000 km and a latitude of 45°, the balance equation has no meaningful solution when $\bar{V}$ is larger than about 47 m/s.

Figures 3 and 4 display selected flow comparisons between various flow quantities obtained by the algebraic approach [Eqs. (10) through (14)] and the same quantities obtained from the balance solution (36). All cases are for $\bar{V}=30$ m/s, $k=2\pi/(6000\text{ km})$, $f=10^{-4}$ s^{-1}, $\beta=1.57\times10^{-11}$ s^{-1} m^{-1}, and the grid consists of a square array, 25 grid points on a side spaced at 250 km.

The geostrophic vorticity (Fig. 3a) of the low pressure centers is about twice as great as the geostrophic vorticity of the high pressure centers, while the vorticity associated with the streamfunction in solution (36) (Fig. 3b) has the same magnitude in low pressure centers as in high pressure centers. This indicates the importance of ageostrophic flow in this case. The vorticity obtained from (13) and (14) (Fig. 3c) and from ξ directly from the algebraic solution of (10) (Fig. 3d) are in much closer agreement with those obtained from the exact solution (36) and with each other than they are with the geostrophic values. The root-mean-square difference between all methods, except the geostrophic, is about 3×10^{-6} s^{-1}.

The u components of motion obtained from (13) and from (36) are shown in Fig. 4a and the v components obtained from (14) and (36) are shown in Fig. 4b. The maximum speeds for the algebraic solutions are about 10% less than those from the boundary value solutions (36) and the root-mean-square difference of the two methods is 1.5 m/s.

b. Rectangular coordinates, non-elliptic data

Specification of $\bar{V}=50$ m/s in (34) renders the balance equation (9) non-elliptic in a region extending several hundred kilometers from the center of anticyclonic circulation. While solution (36) satisfies the balance equation, its physical relevance in the non-elliptic region is doubtful. This solution represents a flow for which the sum of centrifugal, Coriolis, and pressure gradient forces is outward from the center of rotation. It is not possible for such a state to satisfy the condition of zero, steady-state divergence.

However, a divergent steady state solution is a possible limit to a time dependent problem, as described in Section 4. The divergence can be obtained from (32) and the relative vorticity from the resulting condition

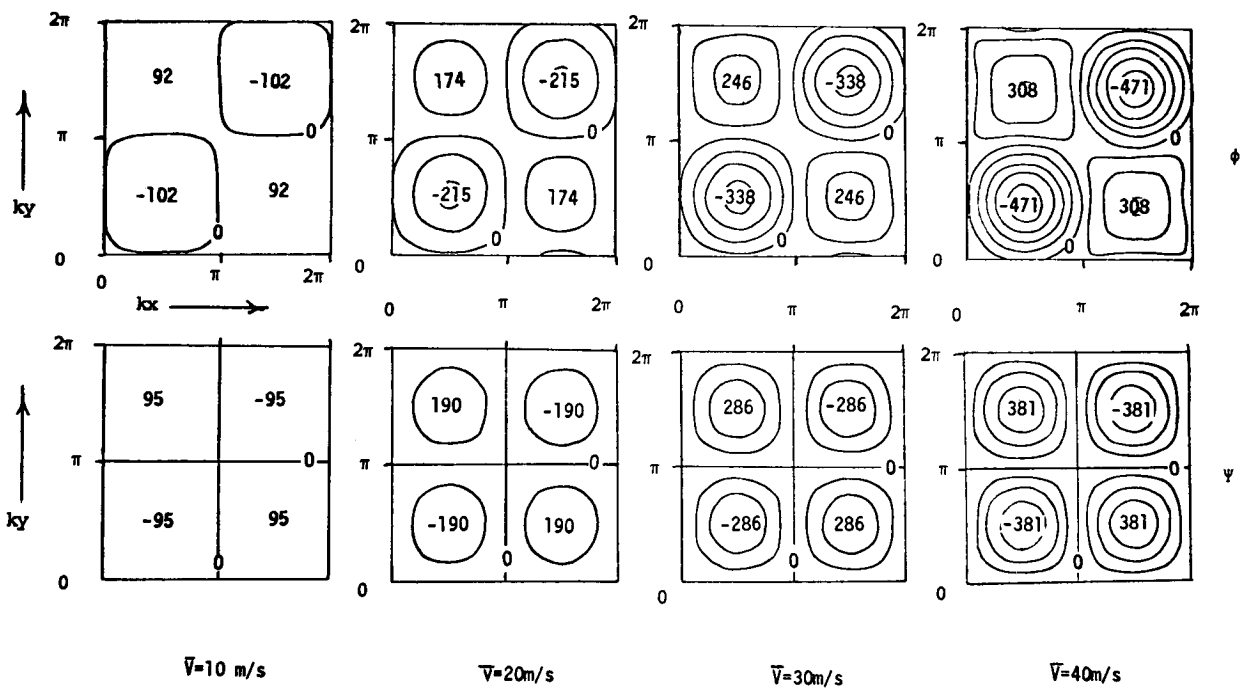

FIG. 2. Analyses of Φ and ψ for indicated values of $\bar{V}$, and $f=10^{-4}$ s^{-1}, $k=2\pi/(6000$ km). Units are 10 m^2/s^2 for Φ and 10^5 m^2/s for ψ. Zero isolines and maxima and minima are indicated. Isoline interval is 100 units.

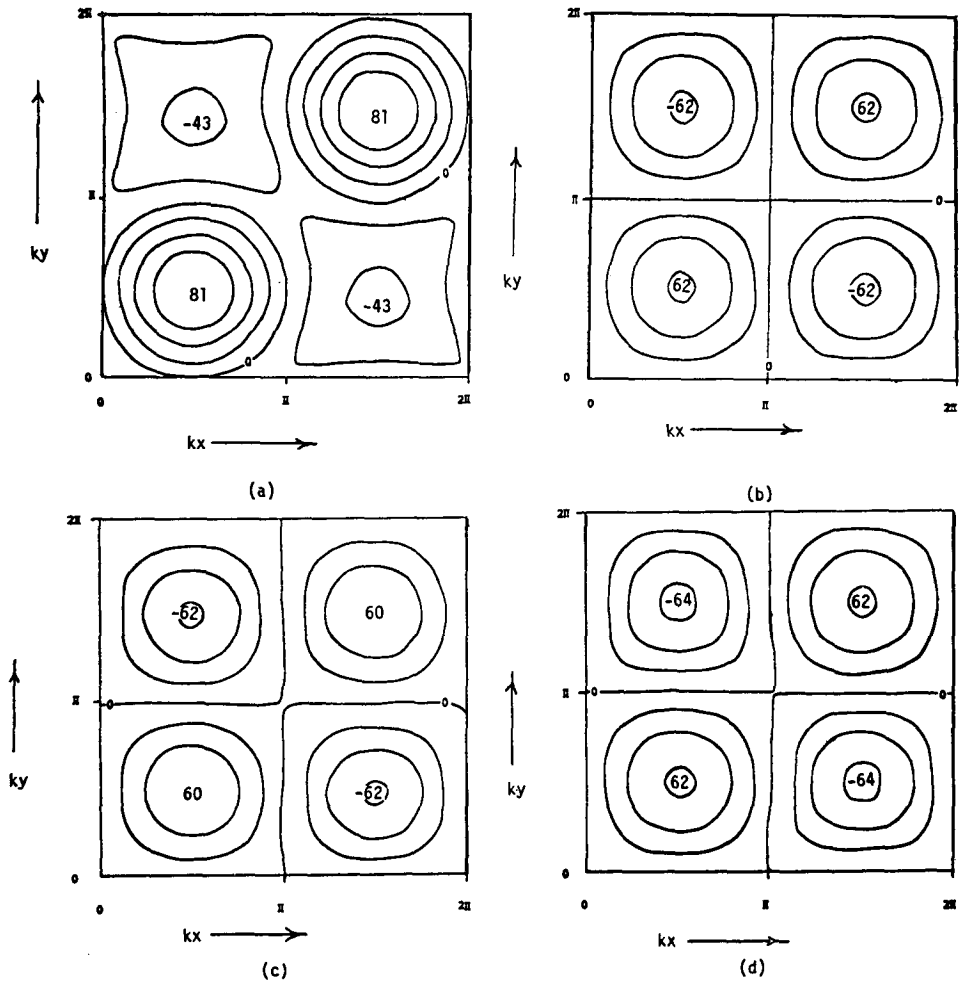

FIG. 3. (a) Geostrophic vorticity (10^{-6} s^{-1}). Isoline interval is 20 units. (b) Relative vorticity obtained from the balance equation. (c) Relative vorticity obtained from the algebraic method, Eqs. (13) and (14). (d) Relative vorticity obtained from the algebraic method, Eq. (10).

that the absolute vorticity must be zero. For the case in which $\bar{V}=50$ m/s, the grid points within about 300 km of the center of highest pressure have divergence of the order of 20×10^{-6} s^{-1}. This is considerably larger than that ordinarily encountered in synoptic-scale motions, and the consequent mass divergence would probably tend to rapidly adjust the pressure pattern to a non-divergent state. The pressure field would not need to undergo substantial change in order to achieve a state where a balanced flow can be non-divergent. Reduction of $\bar{V}$ from 50 m/s to 47 m/s would make such a state possible. Thus, only a relatively small pressure adjustment would be necessary to produce a balanced state, and it is questionable whether any significant "non-elliptic" pressure fields might ever be realized in large-scale flows.

The point can also be reversed: given the fact that only a small pressure rise may be required to produce strong synoptic scale divergence, it is conceivable that strong divergence may be present whenever some mechanism exists to increase pressures only slightly in anticyclonic systems with rotation of the order of the Coriolis parameter.

Miyakoda (1957) has speculated that these pressure increases could be observed in the atmosphere in the cases of intense outbursts from anticyclones, as reported by Syōno (1948).

Strong anticyclonic rotation is often noted on daily weather maps of the 200-mb and 300-mb levels. For example, Krishnamurti (1970) reports extreme values of 200-mb relative anticyclonic vorticity usually reaching values of 10^{-4} s^{-1} in the latitude belt 45°N to 20°S. Except at the northernmost boundary of this region, the magnitude of f is smaller than this. His data also suggest that the anticyclones tend to be climatologically associated with divergence. This is consistent with the results presented in this section.

c. Real data experiments on a spherical grid

The continuous pressure field (34) is composed of relatively long wave components for which truncation

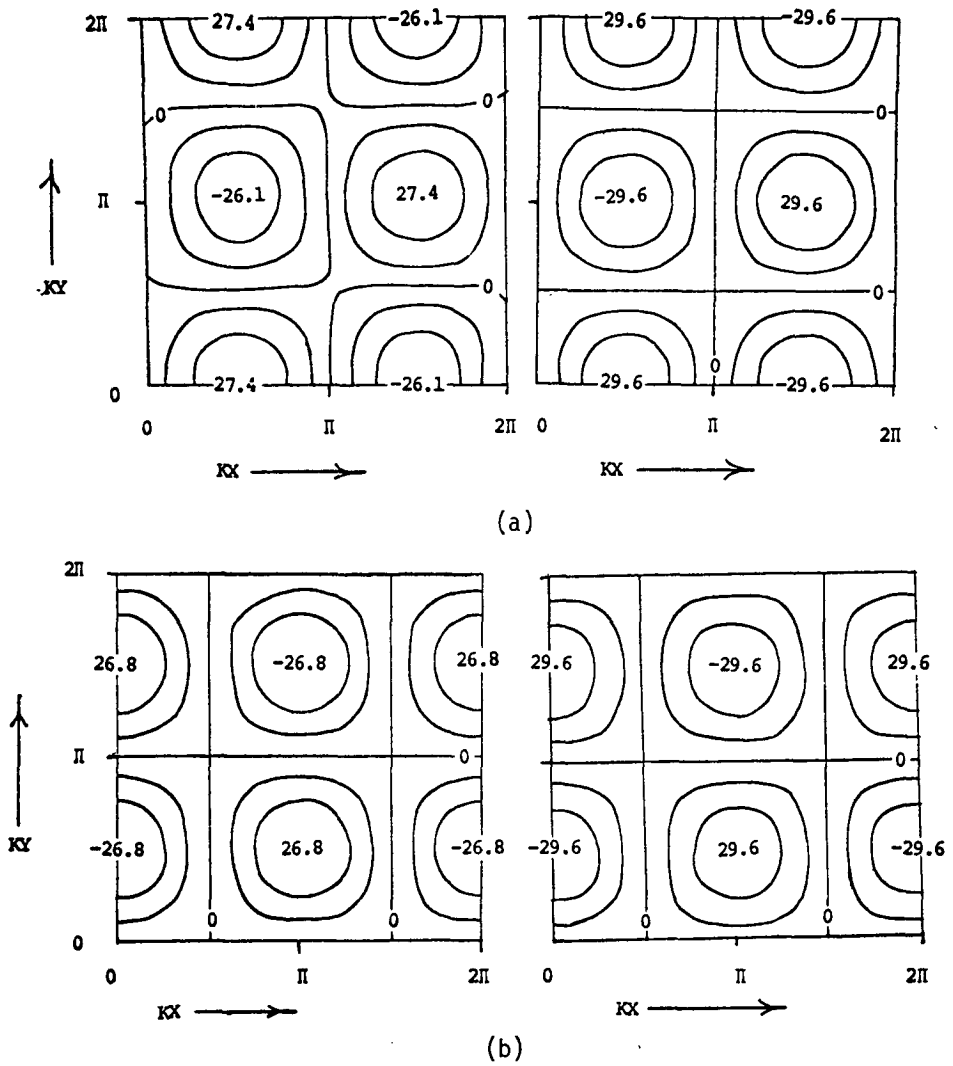

FIG. 4. (a) The u component of velocity obtained from the balance equation (right) and from the algebraic method (left) in m/s. Isoline interval is 10 m/s. (b) The v component of velocity obtained from the balance equation (right) and from the algebraic method (left) in m/s. Isoline interval is 10 m/s.

errors are unimportant, while the magnitude of the nonlinearity can be easily adjusted with parameter $\bar{V}$. This makes (34) a useful tool with which to investigate the basic capabilities of the approach. Actual data cases, of course, have non-zero amplitudes in short as well as long waves and must take account of the earth's sphericity as well.

In order to investigate limitations of the approach for real data studies, a series of 13 mid-winter 500-mb cases was used. The grid for these cases extends from 21°N to 81°N and over all longitudes. Other parameters of the runs are

$$f = 10^{-4}\ \text{s}^{-1}$$

$$\beta = 1.57 \times 10^{-11}\ \text{s}^{-1}\ \text{m}^{-1}$$

$\Delta\phi = 3°$ (latitude grid spacing)

$\Delta\lambda = 2.82°$ (longitude grid spacing)

Each of these cases was also solved for the fully nonlinear balance equation solution using a fast Fourier transform, Gauss elimination, iterative procedure that seems to maximize the efficiency of solution (Paegle and Tomlinson, 1974). The iteration of that method was stopped when the balance equation was solved to within an error tolerance such that the resultant vorticity is within about 10^{-6} s^{-1} of the correct value at every point. The height data was "ellipticized" so that a solution could be obtained for the non-divergent case.

The same cases were run using the algebraic algorithm described in Section 3. Table 1 summarizes root-mean-square differences between solutions given by this algorithm, the Paegle and Tomlinson (1974) balance equation solutions, and geostrophic solutions. The algebraic solutions for u and v which are obtained from equations (7) and (8) are not better approximations

TABLE 1. Root-mean-square differences of algebraic solutions obtained from equations (7), (8), and (3) from balanced and geostrophic values.

	RMS (Δu) (m/s)	RMS (Δv) (m/s)	RMS (Δvorticity) (s^{-1})
Balanced	3.3	2.7	1.2×10^{-6}
Geostrophic	3.7	2.6	5×10^{-6}

to the balanced flow than are the geostrophic solutions in this comparison. However, the vorticity computed using the algebraic method agrees much more closely with the balanced vorticity than with the geostrophic vorticity.

Alternatively, u and v can be obtained from the vorticity as given by (15) through (17) for rectangular coordinates. The u and v obtained in this manner are compared with the balance and geostrophic wind components in Table 2. As expected, they are in good agreement with the balanced u and v fields over the entire grid. These values of u and v differ from the balanced values by an order of magnitude less than they differ from the geostrophic values. It remains to be determined which of the values obtained for u and v agrees more closely with real atmospheric observations. Since no reliable streamfunction analyses were available for our real data cases, this could not be assessed. The advantage of obtaining u and v from (7) and (8) is apparent for those cases in which no reliable approximation can be made for the streamfunction at the boundaries of the region under study. This method of solution requires about 10–20% the computer time of methods described by Paegle and Tomlinson (1974), which are, in turn, about five times more efficient than methods based entirely on relaxation. Thus, the proposed method delivers accurate approximations to balanced flows at less than 10% of the computer time required by the standard relaxation procedures.

Divergent balanced solutions could have been computed for those areas for which the pressure data is non-elliptic. Since most of these occurred over the oceans where upper level data analyses are somewhat unreliable, we did not compute such solutions. As noted in Section 4, the rotational part of those solutions would have been the same as the total solutions obtained by first ellipticizing the height field.

6. Concluding comments

A method has been described which can be used to obtain a balanced flow field that is very similar to the solution of the nonlinear balance equation. The main advantages are:

1) It is computationally more efficient than solution of the balance equation.
2) The kinematic properties: divergence, vorticity, and rate of strain are independent of boundary conditions on the flow.
3) It offers physically reasonable solutions for some pressure patterns for which the balance equation has either no physically meaningful solutions, or ones which are difficult to interpret.

The method has not yet been tested for initialization of primitive equation models, but would represent a more reasonable initial guess than the geostrophic condition for any case in which the balance solution would be better. There is no guarantee that the pressure field may not become non-elliptic, and, on these occasions, the proposed method would not be as strongly restricted as the customary balance equation with regard to the initial data it can accommodate.

Perhaps the chief usefulness of the method is as a diagnostic tool. For example, the question of whether high-level friction or excessively strong upper-level high-pressure centers are responsible for the significant amounts of divergence often observed in upper-level flows is of great importance in understanding large-scale dynamics and for numerical simulations. We are pursuing investigations of this type with emphasis on the tropics and subtropics where the relevance of such upper-level divergence to a wide variety of phenomena ranging from cumulus convection to cloud clusters and Hadley circulations is quite apparent.

TABLE 2. Root-mean-square differences of algebraic solutions (obtained as described in Section 5) from balanced and geostrophic values.

	RMS (Δu) (m/s)	RMS (Δv) (m/s)
Balanced	0.5	0.3
Geostrophic	3.7	2.6

Acknowledgments. Robert Jirsek assisted in some of the computations.

Partial support for this research has been provided through NSF Atmospheric Sciences Section Grants GA 28277, GA 40387, and GA 29200.

REFERENCES

A'rnasen, G., 1958: A convergent method for solving the balance equation. *J. Meteor.*, **15**, 220–225.

Førtoft, R., 1962: A numerical method of solving certain partial differential equations of second order. *Geofys. Publikas.*, **24**, 229–239.

Krishnamurti, T. N., 1968: A study of a developing wave cyclone. *Mon. Wea. Rev.*, **96**, 208–217.

——, 1971: Observational study of the tropical upper tropospheric motion field during the Northern Hemisphere summer. *J. Appl. Meteor.*, **10**, 1066–1096.

Miyakoda, K., 1956: On a method of solving the balance equation. *J. Meteor. Soc. Japan*, **34**, 364–367.

Paegle, J., and E. M. Tomlinson, 1974: Solution of the balance equation incorporating Fourier transform and Gauss elimination techniques. Submitted for publication in *Mon. Wea. Rev.*

Shuman, F. G., 1957: Numerical methods in weather prediction: I. The balance equation. *Mon. Wea. Rev.*, **85**, 329–332.

Syōno, S., 1948: On the mechanism of the outburst of cold air from polar cap. (In Japanese.) *J. Meteor. Soc. Japan*, **26**.

Thompson, P. D., 1956: On the theory of large scale disturbances in nongeostrophic flow. *J. Meteor.*, **13**, 251–261.